Matter-wave solitons with a periodic, piecewise-constant scattering length

A. S. Rodrigues,[1] P. G. Kevrekidis,[2] Mason A. Porter,[3] D. J. Frantzeskakis,[4] P. Schmelcher,[5,6] and A. R. Bishop[7]

[1]*Departamento de Física/CFP, Faculdade de Ciências, Universidade do Porto, R. Campo Alegre, 687–4169-007 Porto, Portugal*

[2]*Department of Mathematics and Statistics, University of Massachusetts, Amherst, Massachusetts 01003-4515, USA*

[3]*Oxford Centre for Industrial and Applied Mathematics, Mathematical Institute, University of Oxford, Oxford, OX1 3LB, United Kingdom*

[4]*Department of Physics, University of Athens, Panepistimiopolis, Zografos, Athens 157 84, Greece*

[5]*Theoretische Chemie, Physikalisch-Chemisches Institut, Im Neuenheimer Feld 229, Universität Heidelberg, 69120 Heidelberg, Germany*

[6]*Physikalisches Institut, Universität Heidelberg, Philosophenweg 12, 69120 Heidelberg, Germany*

[7]*Theoretical Division and Center for Nonlinear Studies, Los Alamos National Laboratory, Los Alamos, New Mexico 87545, USA*

Motivated by recent proposals of "collisionally inhomogeneous" Bose-Einstein condensates (BECs), which have a spatially modulated scattering length, we study the existence and stability properties of bright and dark matter-wave solitons of a BEC characterized by a periodic, piecewise-constant scattering length. We use a "stitching" approach to analytically approximate the pertinent solutions of the underlying nonlinear Schrödinger equation by matching the wave function and its derivatives at the interfaces of the nonlinearity coefficient. To accurately quantify the stability of bright and dark solitons, we adapt general tools from the theory of perturbed Hamiltonian systems. We show that stationary solitons must be centered in one of the constant regions of the piecewise-constant nonlinearity. We find both stable and unstable configurations for bright solitons and show that all dark solitons are unstable, with different instability mechanisms that depend on the soliton location. We corroborate our analytical results with numerical computations.

I. INTRODUCTION

In the past few years, the study of solitary-wave structures in atomic physics has received considerable attention, predominantly because of impressive advances in the field of Bose-Einstein condensation [1,2]. These investigations have largely been motivated by the comprehensive mean-field description of atomic Bose-Einstein condensates (BECs) by the Gross-Pitaevskii (GP) equation, a variant of the nonlinear Schrödinger (NLS) equation in which nonlinearity, whose strength is proportional to the *s*-wave scattering length, is introduced by the interatomic interactions. This remarkable feature has allowed both theoretical investigations and experimental observations of bright [3–5], dark [6–9], and gap [10] matter-wave solitons in BECs (see also the recent review in [11]). Such solitons have been studied in detail in the literature in the presence of various external potentials, including harmonic traps and periodic lattices. This has yielded tremendous insights into a large variety of interesting phenomena, including Bloch oscillations, Landau-Zener tunneling, modulational ("dynamical") instabilities, gap excitations, and more (see the reviews in [11–15] and references therein). The types of matter-wave solitons that arise in a given situation depend on the nature of the interatomic interactions, which, in turn, are characterized by the sign of the scattering length. Specifically, bright solitons arise in BECs with attractive interactions and negative scattering length, whereas dark and gap solitons emerge in the case of repulsive interactions and positive scattering length. Gap solitons also require the presence of an optical lattice or superlattice potential.

During the past decade of BEC research, a number of tools have been developed to control and manipulate matter

waves. For example, they can be influenced, processed, and shaped using static (homogeneous and inhomogeneous) electric and magnetic fields [16], optical devices [17], and near-field radio-frequency devices [18]. One can manipulate not only a BEC's external (trapping) potential, but also the interactions among the atoms that are responsible for the nonlinear properties and dynamics of the matter waves. The interaction among ultracold atoms can be adjusted in a very broad range experimentally by employing either magnetic [19,20] or optical Feshbach resonances [21]. Additionally, so-called "confinement-induced resonances" [22,23] allow one to vary the effective one-dimensional (1D) coupling constant of quasi-1D systems by adjusting the transversal confinement length. One can consequently vary the external potential while independently and simultaneously changing the strength of the nonlinearity by tuning the interatomic interactions.

The manipulation of BECs using Feshbach resonances has propelled a significant number of investigations that have been subsequently refined substantially. Experimental achievements include the formation of bright matter-wave solitons and soliton trains for ^{7}Li [3,4] and ^{85}Rb [5] atoms by tuning the interatomic interaction within a stable BEC from repulsive to attractive, the formation of molecular condensates [24], and the probing of the BEC-BCS crossover [25]. Moreover, theoretical studies have predicted that a time-dependent modulation of the scattering length can be used to stabilize attractive two-dimensional BECs against collapse [26] or create robust matter-wave breathers in 1D BECs [27]. We remark in passing that relevant contexts involving the dependence of the nonlinearity coefficient on the evolution variable have also been of interest in nonlinear optics in describing pulse propagation in an optical fiber in the presence

of periodically varying dispersion and nonlinearity [28,29] (see also the references therein). A popular approach has been to look for an averaged (over the fast variation scale) equation with constant coefficients in which solitary-wave solutions could be sought. This approach has also been useful in the context of BECs in describing the averaged properties of solitary waves in the presence of a periodic, time-dependent modulation of the scattering length [30–32].

In addition to the aforementioned studies involving temporal variations of the interaction strength, it has been recently found that atomic matter waves exhibit novel features under the influence of a spatially varying scattering length and, consequently, a spatially varying nonlinearity. The resulting so-called "collisionally inhomogeneous" environment provides a variety of interesting and previously unexplored dynamical phenomena and potential applications, including adiabatic compression of matter waves [33,34], atomic soliton emission and atom lasers [35], enhancement of the transmittivity of matter waves through barriers [36,37], dynamical trapping of matter-wave solitons [36], stable condensates exhibiting both attractive and repulsive interatomic interactions [38], and the delocalization transition of matter waves [39]. Particular inhomogeneous frameworks that have been investigated include linear [33,36], parabolic [40], random [41], periodic [39,42,43], and localized (steplike) [35,44,45] spatial variations. There have also been a number of detailed mathematical studies [46–48]. In particular, Refs. [46,47] examined the effects of a "nonlinear lattice potential" (i.e., a spatially periodic nonlinearity coefficient) on the stability and instability of solitary waves and elucidated the interplay between drift or diffraction and blowup instabilities. More recently, the interplay of nonlinear and linear potentials has been examined in both continuum [49] and discrete [50] settings.

Motivated by the above studies, as well as the suggestion of a piecewise-constant inhomogeneous scattering length in Refs. [35,45], we investigate in the present work matter-wave solitons in the framework of the NLS equation with a periodic, piecewise-constant nonlinearity coefficient. Preparing such a setup experimentally is challenging, but possible in principle. For example, it could be achieved by integrating optical and magnetic traps on an atom chip [16]. The underlying idea is as follows: an on-chip fiber-optic configuration generates a microscopic dipole waveguide with a strong transversal confinement [51]. This waveguide is augmented by a periodic array of either permanent magnets [52] or current-carrying wires [16] that create alternating zones of approximately zero and constant magnetic fields in the longitudinal direction. Tuning the magnetic field (via, for example, the currents in the wires) such that the resulting field strength leads to an atomic scattering process close to a Feshbach resonance allows one to achieve a substantial variation of the atomic scattering behavior in the form of an alternating, approximately piecewise-constant scattering length. References [35,45] considered a localized region with positive scattering length (the rest of the BEC was noninteracting, providing a substantial linear regime). Here, however, we consider a scattering length given by a piecewise-constant function that switches periodically between either two positive or two negative values. The importance of this particular

fully nonlinear setting is that it allows us to analytically investigate the existence and stability of matter-wave solitons in each region (where the nonlinearity coefficient is constant) and to subsequently "stitch" the constructed (local) solutions at the jump points of the piecewise-constant nonlinearity function. Our analysis is similar in spirit to the approach used in a situation with both linear and nonlinear, piecewise-constant periodicity in Ref. [53]. We employ techniques from the general theory of perturbed Hamiltonian systems, starting from the unperturbed limit of the completely integrable 1D NLS equation, in order to analytically address the stability of both bright [54] and dark [55] matter-wave solitons. In order to quantify the accuracy of our theoretical predictions, we subsequently compare these findings with direct numerical computations.

Our presentation is organized as follows. In Sec. II, we present our setup and the pertinent GP model. We study bright and dark matter-wave solitons, respectively, in Secs. III and IV. Finally, in Sec. V, we briefly summarize our findings and present our conclusions.

II. SETUP AND MODEL

We consider a "cigar-shaped" condensate that is elongated along the z direction and strongly confined in the transverse (x and y) directions. Assuming that this condensate is collisionally inhomogeneous, characterized by a spatially varying scattering length $a(z)$, we follow the standard approach [56] of averaging the 3D GP equation in the transverse plane. We thereby arrive at the following 1D GP equation for the longitudinal wave function $\psi(z,t)$:

$$i\hbar \partial_t \psi(z,t) = \left[-\frac{\hbar^2}{2m}\partial_z^2 + 2\hbar\omega_\perp a(z)|\psi(z,t)|^2 \right]\psi(z,t), \quad (1)$$

where m is the atomic mass and $\omega_\perp$ is the transverse confinement frequency.

Measuring time and space in units of $\omega_\perp^{-1}$ and transverse oscillator length $l_\perp \equiv \sqrt{\hbar/m\omega_\perp}$, respectively, we reduce the GP equation (1) to the dimensionless form

$$i\partial_t \phi(z,t) = \left[-\frac{1}{2}\partial_z^2 + g(z)|\phi(z,t)|^2 \right]\phi(z,t), \quad (2)$$

where $\phi(z) = \sqrt{2|a_0|}\psi(z)$ and $g(z) = a(z)/|a_0|$ is negative (positive) for attractive (repulsive) interatomic interactions. In the above expressions, a_0 denotes the value of the scattering length of the corresponding collisionally homogeneous system, for which $g(z) = g_0 = $ const. Note that Eq. (2) has the form of a 1D NLS equation. It possesses two integrals of motion: the normalized number of atoms, $N = \int_{-\infty}^{+\infty}|\phi|^2 dz$, and the Hamiltonian. The former is connected to the unnormalized number of atoms $\mathcal{N}$ through the equation $\mathcal{N} = (a_\perp/2|a_0|)N$.

We take the nonlinearity coefficient $g(z)$ in Eq. (2) to be a piecewise-constant function of space:

$$g(z) = \begin{cases} g_0, & \text{if } 0 < \text{mod}(z,L) < L_1, \\ g_1, & \text{if } L_1 < \text{mod}(z,L) < L. \end{cases} \quad (3)$$

Note that the nonlinearity coefficient in Eq. (3) may also be expressed as $g(z) = g_0 + \Delta g(z)$, where

$$\Delta g(z) = \Delta g_0 \sum_{n=-\infty}^{n=+\infty} \{\Theta(z - [nL + L_1]) - \Theta(z - [n+1]L)\},$$

$$(4)$$

where $\Delta g_0 = g_1 - g_0$ and Θ is the Heaviside step function.

In our numerical investigations (see the discussion below), we adopt values of the parameters that are typical for experimental setups. In particular, we consider a quasi-1D trap with a transverse confining frequency $\omega_\perp = 2\pi \times 1400$Hz, which fixes the temporal unit to 0.1ms. We assume that the dimensionless chemical potential μ is of order $O(1)$. For an (attractive) ^{7}Li condensate, this choice yields a spatial unit of 1μm and a number of atoms of $N \approx 1100$. For the (repulsive) ^{87}Rb (respectively, ^{23}Na) condensate, this yields a spatial unit of 0.3 μm (2.2 μm) and a number of atoms of $N \approx 1200$ (16 000). Moreover, we assume that the nonlinearity function $g(z)$ is characterized by changes Δg of the order of 50% of the typical values of the scattering lengths and that the normalized periodicity L is of the order $O(1)$ (i.e., it is about a few microns). This choice is consistent with typical Feshbach resonances that occur in Li, Rb, and Na condensates: changing the magnetic field by a factor of 2 on a micron scale in the neighborhood of a Feshbach resonance requires magnetic field gradients in the range 1–100 kG/cm, which are of moderate size for atom chips. The lower limit is also compatible with the gradients used in macroscopic trap setups.

Below, we will quantify the existence and stability properties of bright and dark matter-wave solitons [for negative and positive nonlinearity coefficients $g(z)$, respectively] as a function of the inhomogeneity strength Δg_0.

III. BRIGHT MATTER-WAVE SOLITONS

A. Perturbation analysis

Let us first consider an attractive BEC characterized by a negative nonlinearity coefficient in Eq. (2), so that $g_0 < 0$ and $|\Delta g(z)| < |g_0|$. In the special case of a homogeneous nonlinearity, scaled such that its coefficient is $g_0 = -1$, Eq. (2) possesses a bright matter-wave soliton solution of the form

$$\phi_{bs}(z,t) = \eta \, \text{sech}[\eta(z - z_0)]\exp(i\mu t),$$

$$(5)$$

where η is the soliton's amplitude and inverse width, z_0 is the position of its center, and $\mu = -(1/2)\eta^2$ is its effective chemical potential. We then consider the spatial inhomogeneity as a perturbation of strength $\epsilon \equiv \Delta g_0$. When $\epsilon \neq 0$, the integrability of the original NLS equation (2) is lost, but the system is still Hamiltonian. Its Hamiltonian functional is given by $H = H_0 + \epsilon H_1$, where the unperturbed (H_0) and perturbed (H_1) parts of the Hamiltonian are given by

$$H_0 = \int_{-\infty}^{+\infty} \frac{1}{2}(|\partial_z \phi|^2 - |\phi|^4)dz,$$

$$(6)$$

$$H_1 = \int_{-\infty}^{+\infty} \frac{1}{2}\frac{\Delta g(z)}{\Delta g_0}|\phi|^4 dz.$$

$$(7)$$

In accordance with the general perturbation theory for Hamiltonian systems developed in Ref. [54], the condition for the existence of the solution (5) under the aforementioned perturbation is that it remains an extremum of the perturbation Hamiltonian H_1. In the present case, it is easy to see by considering the dependence of H_1 on z_0 that this condition is satisfied provided z_0 is either at the center of a region with nonlinearity coefficient g_0 or (by symmetry) at the center of a region with nonlinearity coefficient g_1. Therefore, we can identify stationary solitary-wave solutions centered at these points in the presence of the periodic, piecewise-constant nonlinearity.

Let us consider the stability of these bright matter-wave solitons. As is well known, the unperturbed NLS equation is invariant under both translation and phase or gauge transformations. If the perturbation is sufficiently small, instability can arise in the case of attractive nonlinearity only via the perturbation-induced breaking of one of these symmetries. (Note that the continuous spectrum is bounded away from the origin and for small ϵ cannot give rise to an instability [54].) Furthermore, it is clear that in the presence of a spatially dependent nonlinearity, the U(1) symmetry (i.e., the phase invariance) of the equation is preserved, so the stability ultimately should depend on the location of the translational eigenvalue. The eigenvalues λ (and the corresponding eigenfrequencies ω, which satisfy $\omega^2 = -\lambda^2$) can be obtained within the framework of the perturbation analysis of Hamiltonian systems in Ref. [54] (see also Ref. [40]) according to the equation

$$\det(\epsilon \mathbf{M} - \omega^2 D) = 0,$$

$$(8)$$

where the matrices $\mathbf{M}$ and $\mathbf{D}$ are given by

$$\mathbf{M} = \begin{pmatrix} \frac{\partial}{\partial z_0}\left\langle \frac{\delta H_1}{\delta \phi^*}, \frac{\partial \phi_{bs}}{\partial z_0} \right\rangle & 0 \\ 0 & 0 \end{pmatrix},$$

$$(9)$$

$$\mathbf{D} = \begin{pmatrix} \left\langle \frac{\partial \phi_{bs}}{\partial z}, -z\phi_{bs} \right\rangle & 0 \\ 0 & -\left\langle \phi_{bs}, \frac{\partial \phi_{bs}}{\partial \eta} \right\rangle \end{pmatrix}.$$

$$(10)$$

In the above equations, the asterisk (*) denotes complex conjugation, $\langle \cdot, \cdot \rangle$ denotes the inner product, and $\delta H_1 / \delta \phi^*$ is the functional (Fréchet) derivative.

The nonzero elements of the matrices $\mathbf{M}$ and $\mathbf{D}$ (i.e., m_{11}, d_{11}, and d_{22}) can then be calculated directly to obtain

$$m_{11} = -\eta^5 \sum_{n=-\infty}^{n=+\infty} \{\sinh[\eta([n+1]L - z_0)]$$

$$\times \text{sech}^5[\eta([n+1]L - z_0)] - \sinh[\eta(L_1 + nL - z_0)]$$

$$\times \text{sech}^5[\eta(L_1 + nL - z_0)]\},$$

$$(11)$$

while

$$d_{11} = \eta \quad \text{and} \quad d_{22} = -1/\eta. \tag{12}$$

Equation (8) allows one to calculate the translational eigenfrequencies to leading order in ϵ, yielding

$$\epsilon m_{11} - \omega^2 \eta = 0. \tag{13}$$

The sum in Eq. (11) can then be calculated numerically. Note that this sum converges rapidly because its component functions decay exponentially, and only three terms ($n=-1$, 0, and $+1$) are needed to obtain a value that is accurate up to ten digits. Below we will directly compare the analytical prediction provided by Eq. (13) to the numerical results for different values of Δg_0 (and of the soliton's chemical potential μ) obtained by computations.

B. "Stitching" of bright soliton solutions

We can use specific features of this particular system to go beyond the above theory, which is valid for general perturbed Hamiltonian systems, and acquire a quantitative handle on the perturbed soliton profile. In particular, we use the fact that one can explicitly construct the solution of the steady-state equation for each of the regions in which the nonlinear coefficient is constant. For sufficiently small ϵ, we expect the solutions to deviate little from the solution ϕ_{bs}. We then construct an analytical approximation to the perturbed solution by "stitching" together the functions that would be solutions to the respective homogeneous NLS equations, with the nonlinearity coefficients taking different constant values in different spatial regions. To do this, we require that the wave function ϕ and its first spatial derivative $\partial_z \phi$ be continuous across the boundaries between regions of different g.

Let us consider, in particular, the bright soliton solution of Eq. (2) centered at z_m with amplitude η_m in a region with nonlinearity coefficient g_m:

$$\phi_m(z) = \frac{\eta_m}{\sqrt{g_m}} \text{sech}[\eta_m(z - z_m)]. \tag{14}$$

Starting with a known value of, say, η_m and z_m, we then need to calculate all other η_j and z_j ($j \neq m$) as a function of the known ones. Applying the aforementioned continuity conditions, we obtain

$$\frac{\eta_m}{\sqrt{g_m}} \text{sech}[\eta_m(Z_m - z_m)] = \frac{\eta_{m+1}}{\sqrt{g_{m+1}}} \text{sech}[\eta_{m+1}(Z_m - z_{m+1})], \tag{15}$$

$$-\frac{\eta_m^2}{\sqrt{g_m}} \text{sech}[\eta_m(Z_m - z_m)] \tanh[\eta_m(Z_m - z_m)]$$
$$= -\frac{\eta_{m+1}^2}{\sqrt{g_{m+1}}} \text{sech}[\eta_{m+1}(Z_m - z_{m+1})] \tanh[\eta_{m+1}(Z_m - z_{m+1})], \tag{16}$$

where Z_m is the coordinate of the interface between regions m and $m+1$. Using Eq. (15), it is then possible to simplify Eq. (16) to get

$$\eta_{m+1}(Z_m - z_{m+1}) = \text{arctanh}\left\{ \frac{\eta_m}{\eta_{m+1}} \tanh[\eta_m(Z_m - z_m)] \right\},$$

from which we obtain z_{m+1} once η_{m+1} is known. We can then proceed iteratively to obtain (z_{m+2}, η_{m+2}), etc. Note, however, that this method is not exact, as can be inferred by close inspection. In particular, Eqs. (15) and (16) possess two unknowns z_{m+1} and η_{m+1}, provided z_m and η_m are given. However, in principle, the quantity η_{m+1} is determined by the coefficient g_1 of the piecewise-constant nonlinearity (and the chemical potential μ). Hence, the system is, in fact, overdetermined. Nevertheless, as long as μ is not too small [so that the width of the soliton is smaller than or comparable to the size of a step in the periodic nonlinearity (see Fig. 1)], the above stitching procedure is fairly accurate, as will be discussed below when we present the results of our numerical simulations.

C. Numerical results

We begin the description of our numerical findings by illustrating the solution obtained by numerically solving the standing-wave problem corresponding to Eq. (2) via a fixed point (Newton-Raphson) iteration. In Fig. 1, we show an example of both a stable bright matter-wave soliton solution (top left) and an unstable one (bottom left). We also present (in the right panels of the figure) the corresponding spectral planes $[\text{Re}(\omega), \text{Im}(\omega)]$ of the eigenfrequencies $\omega = \text{Re}(\omega) + i \text{Im}(\omega)$ that result from a Bogoliubov–de Gennes analysis of the NLS equation around the soliton solution. The absence of eigenfrequencies with nonzero imaginary part indicates stability, whereas the presence of imaginary or complex eigenfrequencies is a signature of linear instability. The stability features observed are reminiscent of the ones found in earlier works, such as Refs. [46,47,49]. Namely, the solution is stable when centered at a maximum of the magnitude of the piecewise-constant, periodic nonlinearity, but it is linearly unstable when centered at a minimum. In Fig. 1, we also show the solutions that we obtained semianalytically via the "stitching" procedure illustrated above. Observe the excellent agreement between those solutions and those computed using fully numerical simulations. In fact, the two solutions are virtually indistinguishable in this case and, more generally, in all situations with sufficiently large $|\mu|$.

Figure 2 depicts the evolution of bright matter-wave solitons with initial configurations of the forms presented in Fig. 1. In particular, we present the stable case (which has parameter values $\mu = -1.0$ and $\Delta g_0 = +0.5$) in the top panel. Observe that the bright soliton remains unchanged during the evolution, as predicted by the linear stability analysis. On the other hand, we show the unstable case (with parameter values $\mu = -1.0$ and $\Delta g_0 = -0.5$) in the bottom panel. Observe that for $t \gtrsim 80$, the soliton drifts [46,47,49] and starts oscillating around a stable fixed point (the center of a neighboring maximum of the magnitude of the periodic potential) as a result of the existence of the imaginary eigenfrequency.

In Fig. 3, we show a conclusive diagram that summarizes our results for the linear stability of the bright-soliton solutions we constructed. The plot shows the relevant transla-
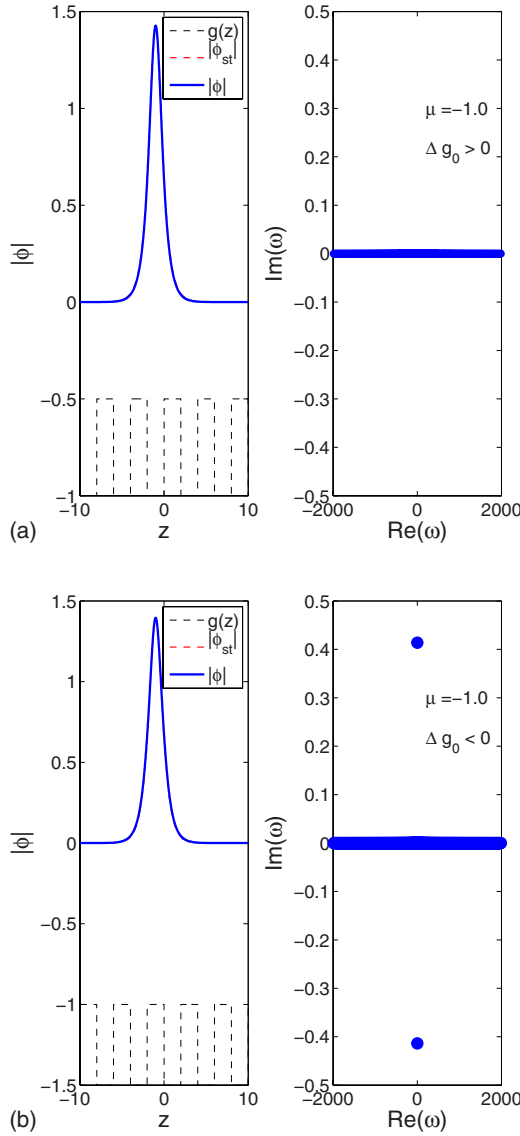
(a)

(b)

FIG. 1. (Color online) Stitched bright-soliton solutions versus fully numerical bright-soliton solutions of the NLS equation. The top left panel shows the wave profile and the "stitched" solution for the same parameter values ($\mu = -1.0$ and $\Delta g > 0$). The top right panel gives the corresponding spectral plane $(\mathrm{Re}(\omega), \mathrm{Im}(\omega))$ of the eigenfrequencies $\omega = \mathrm{Re}(\omega) + i\,\mathrm{Im}(\omega)$. In the bottom panels, we show the same plots for a case with $\mu = -1$ and $\Delta g < 0$. The dashed curves in the left panels show the spatially dependent nonlinearity coefficients. The bright soliton depicted in the top panels is stable, whereas that in the bottom panels is unstable. Notice that for these parameters the stitched solution is practically indistinguishable from the numerically exact one.

tional (squared) eigenfrequency as a function of the strength of the perturbation Δg_0 for different values of the frequency μ. It is clear that the corresponding squared eigenfrequency is essentially linear in Δg_0, giving rise to instability for $\Delta g_0 < 0$ and stability for $\Delta g_0 > 0$. In all cases, we observe very good agreement between the theoretical prediction and the numerical results, especially when Δg_0 is sufficiently small (for which we expect the theory to be most accurate).
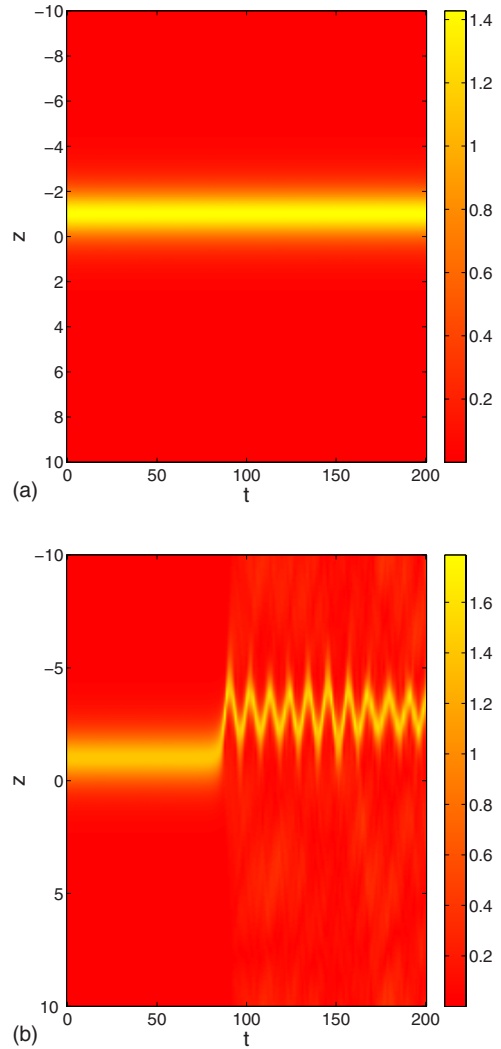
FIG. 2. (Color online) Time evolution of the bright matter-wave soliton for the two cases shown in Fig. 1. The top panel shows the contour plot of $|\phi(z,t)|$ for parameter values $\mu = -1.0$ and $\Delta g_0 = +0.5$, whereas the bottom one shows the case of $\mu = -1.0$ and $\Delta g_0 = -0.5$. The bright soliton depicted in the top panel remains unchanged during the evolution, whereas that in the bottom panel drifts after $t \gtrsim 80$ and oscillates around a stable equilibrium point [i.e., around a maximum of $|g(z)|$].

IV. DARK MATTER-WAVE SOLITONS

A. Perturbation analysis

We now consider repulsive BECs, which are characterized by a positive nonlinearity coefficient in Eq. (2). That is, $g_0 > 0$, with $|\Delta g(z)| < g_0$ as in the previous case. In the special case of a homogeneous nonlinearity, scaled so that its coefficient is $g_0 = +1$, Eq. (2) possesses a dark (black) matter-wave soliton solution of the form

$$\phi_{ds}(z,t) = \eta \tanh[\eta(z - z_0)]\exp(i\mu t), \qquad (17)$$

where η is the soliton's amplitude and inverse width, z_0 is its center position, and $\mu = \eta^2$ is its effective chemical potential. In the case under consideration, the solution (17) has non-vanishing boundary conditions at infinity, with the
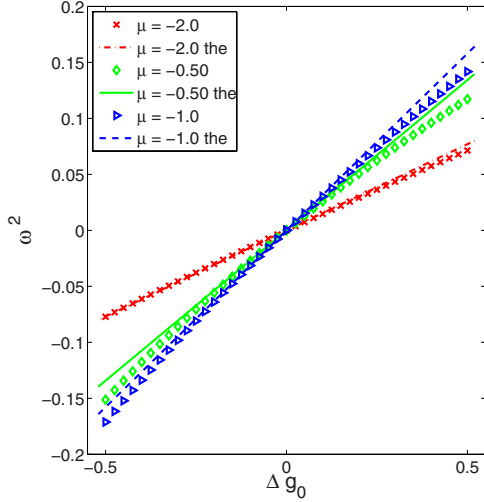
FIG. 3. (Color online) Numerical results (points) and theoretical predictions resulting from the perturbation analysis (curves, which are labeled "the" in the inset) for the translational squared eigenfrequency ω^2 as a function of perturbation strength Δg_0 for different values of the effective chemical potential μ of the bright matter-wave soliton.

asymptotic limits $\phi_{ds}(z) \to \pm \eta$ as $z \to \pm \infty$. Consequently, one can cast the problem of the piecewise-constant nonlinearity in the form of a perturbation, reminiscent of what was done for linear external potentials in Ref. [55]. The perturbed part of the Hamiltonian can be written formally as

$$H_1 = \frac{1}{4} \int \frac{\Delta g(z)}{\Delta g_0} [\eta^4 - \phi^4(z)] dz. \tag{18}$$

We remark that for the perturbed solutions (see the relevant figures in the numerical section below), it is not obvious that this integral converges. However, for the unperturbed solution (for which the solvability condition under the effect of perturbation is applied), it is certainly convergent.

Following Ref. [55], one can show in a straightforward manner that for the solution to survive under the effect of perturbation (using the perturbation parameter $\epsilon \equiv \Delta g_0$), the function

$$M'(s) = \frac{1}{2} \int_{-\infty}^{+\infty} \frac{d\Delta g}{dz}(z) [\eta^4 - \phi_0^4(z - s)] dz \tag{19}$$

must vanish. As was the case for the bright matter-wave solitons we analyzed in the previous section, this condition implies that the center of the dark matter-wave soliton must be located at the center of either a region in which the nonlinearity coefficient is g_0 or at the center of one in which it is g_1.

The stability of the dark-soliton solution we constructed depends on the sign of the second derivative of $M(s)$ evaluated at the root s_0 of the first derivative (19). Based on the analysis of Ref. [55], an instability will be present with one imaginary eigenfrequency pair if $\epsilon M''(s_0) < 0$ and with exactly one complex eigenfrequency quartet if $\epsilon M''(s_0) > 0$. As was the case for bright solitons (but with some important differences, which we discuss below), this instability is dic-

tated by the translational eigenvalue, which needs to bifurcate from the origin as soon as the perturbation is present. For $\epsilon M''(s_0) < 0$, the relevant eigenfrequency pair moves along the imaginary axis, leading to an immediate instability associated with exponential growth of a perturbation along the associated eigendirection. For $\epsilon M''(s_0) > 0$, on the other hand, the eigenfrequency moves in principle along the real axis, which, however, is filled with a continuous spectrum. Consequently, as a result of the opposite signature (to these eigenfrequencies) of the translation mode, the eigenfrequency exists as a complex quartet, signaling the presence of an oscillatory instability. In fact, following Ref. [55], we find that the relevant eigenfrequencies are determined by the characteristic equation

$$\lambda^2 + \frac{\epsilon}{4} M''(s_0) \left(1 - \frac{\lambda}{2} \right) = O(\epsilon^2), \tag{20}$$

where the perturbation is given by Eq. (4) and we recall that the eigenvalues λ are related to the eigenfrequencies ω through $\lambda^2 = -\omega^2$.

Because the two roots of $M'(s)$ are $s_{01} = nL + L_1/2$ and $s_{02} = nL + L_1 + L/2$, one can evaluate $M''(s_0)$ explicitly to obtain

$$M''(s_{01}) = 4\eta^5 \sum_{p=-\infty}^{p=+\infty} \left\{ \tanh^3 \left[\eta \left(pL + \frac{L_1}{2} \right) \right] \right.$$
$$\left. - \tanh^5 \left[\eta \left(pL + \frac{L_1}{2} \right) \right] \right\} \tag{21}$$

and a similar expression for $M''(s_{02})$. Combining Eqs. (20) and (21) yields a prediction for the location of the relevant translational eigenfrequency. We now turn to numerical simulations in order to examine the accuracy of our analytical results.

B. Numerical results

In Fig. 4, we show the profile and spectral plane of the dark matter-wave soliton when it is centered at $\min[g(z)]$ (top panels) and $\max[g(z)]$ (bottom panels). The former case is associated with the scenario in which $\epsilon M''(s_0) > 0$ and its corresponding spectral plane has an eigenvalue quartet (corresponding to an oscillatory instability). The latter case is characterized by $\epsilon M''(s_0) < 0$, which results in a real eigenvalue (imaginary eigenfrequency) pair in the spectral plane.

Figure 5 depicts the evolution of dark solitons with the two initial configurations shown in Fig. 4. In both cases, $\mu = 1$ and $|\Delta g_0| = 0.5$. In the top panel, the wave is centered at $\min[g(z)]$, and in the bottom panel, it is centered at $\max[g(z)]$. Unlike their bright counterparts, dark solitons become mobile (unstable) in both cases. This mobility develops earlier for the soliton in the bottom panel because its eigenfrequency has a much larger imaginary part than that of the soliton in the top panel. Furthermore, in the top configuration, the instability is initiated through an oscillatory phase that stems from its complex eigenfrequency quartet. This feature is absent in the case of a wave centered at $\max[g(z)]$, as is expected when there is an imaginary eigenfrequency
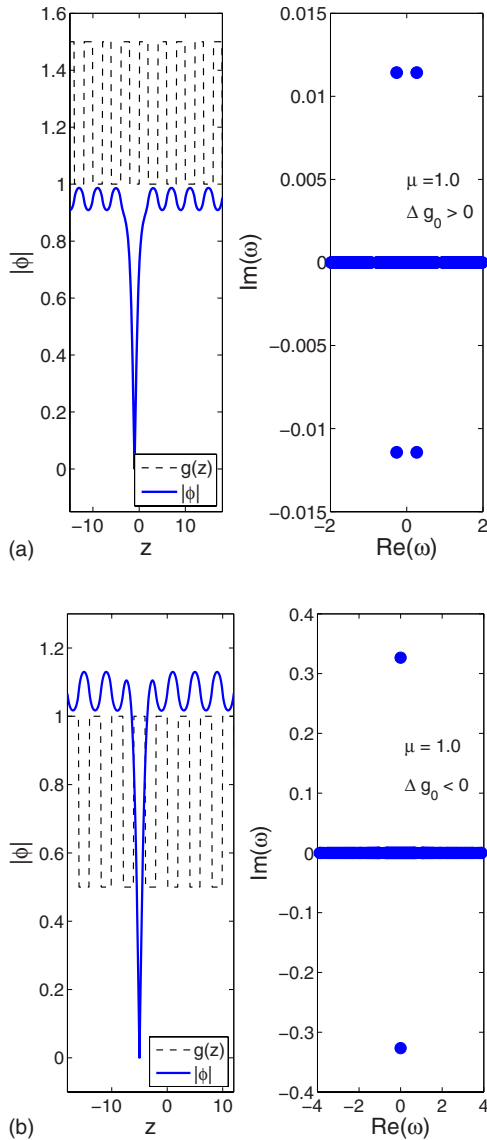
(a)

(b)

FIG. 4. (Color online) Numerical dark matter-wave soliton so-
lutions of the NLS equation (2). The top and bottom left panels
show the wave profiles (solid curves) in the presence of a periodic,
piecewise-constant coefficient in front of the nonlinearity (dashed
curves). In each case, the chemical potential is $\mu=1$. The soliton is
centered at $\min[g(z)]$ in the top panels and at $\max[g(z)]$ in the
bottom ones. The right panels show the eigenfrequency spectrum
(similar to the right panels of Fig. 1). The top panel illustrates an
oscillatory growth due to a complex quartet of eigenfrequencies,
and the bottom shows an exponential growth due to an imaginary
eigenfrequency pair.

pair (which corresponds to a purely exponential instability).
It is interesting to note that in both cases, as the soliton
becomes mobile over the periodically nonlinear terrain, it
radiates (a process that has been discussed elsewhere, al-
though for a linear periodic potential; see, for example, Refs.
[57] and references therein) and is eventually destroyed.

For the $\min[g(z)]$-centered soliton, we compare in the
bottom panel of Fig. 6 the imaginary part of the eigenfre-
quency quartet (which corresponds to the real part of the
eigenvalue quartet and yields the growth rate of the instabil-
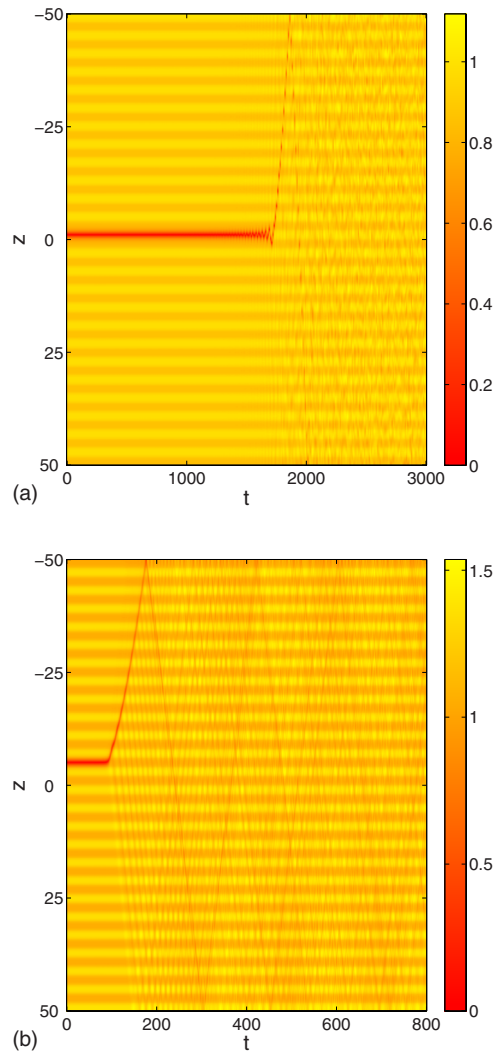

(a)

(b)

FIG. 5. (Color online) Time evolution of the dark soliton for the
two configurations shown in the left panels of Fig. 4. The dark
soliton shown in the top panel remains unchanged for a longer time,
showing evidence of an eigenfrequency with a smaller imaginary
part. Furthermore, the former instability is oscillatory in its initial
stages of development (indicating its association with a complex
eigenfrequency quartet), whereas the latter is not (indicating its con-
nection to an imaginary eigenfrequency).

ity) to the theoretical predictions of Eqs. (20) and (21). Al-
though finite-size effects similar to the ones reported in Ref.
[55] (see the detailed discussion of Ref. [58]) are present, the
agreement between the theoretical prediction and the numeri-
cal result is good (and becomes better as the domain size
increases). We show three numerical cases and observe that
the agreement with the theoretical prediction improves (as
expected) as the density of the numerical phonon band of
eigenvalues increases (for larger domain length L). See Ref.
[58] for details on this finite-size effect. We also show the
real part of the corresponding eigenfrequency for different
domain lengths, for which the change in domain size does
not play such a significant role. As shown in Fig. 7, we
observe a similar level of agreement (but without the finite-
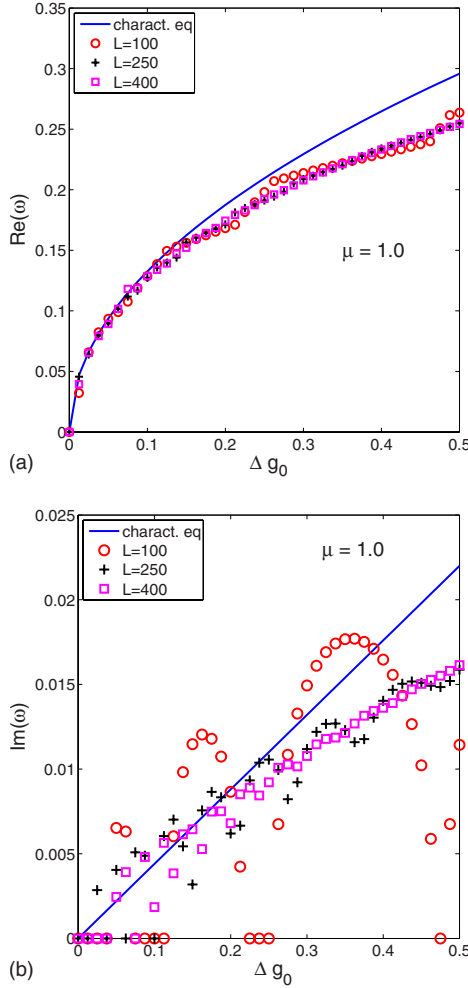size effects, because the relevant eigenfrequency is now

FIG. 7. (Color online) Imaginary part of the eigenfrequency as a function of the perturbation strength Δg_0 for a BEC with chemical potential $\mu = 1.0$ which has a soliton centered at $\max[g(z)]$. The solid curve and the points correspond, respectively, to the analytical prediction and the numerical result for the imaginary eigenfrequency.

FIG. 6. (Color online) Real (top panel) and imaginary (bottom panel) parts of the eigenfrequency as a function of perturbation strength Δg_0 for a BEC with a chemical potential of $\mu = 1.0$ which has a soliton centered at $\min[g(z)]$. The points give the numerical results and the solid curve gives the theoretical prediction for the real and imaginary parts of the complex eigenfrequency quartet. In both panels, we present the results of numerical simulations for three different domain sizes L in order to illustrate the role of the finite size of the computational lattice, which is especially evident in the instability growth rate represented by $\text{Im}(\omega)$.

imaginary) for a $\max[g(z)]$-centered dark soliton [for which $\epsilon M''(s_0) < 0$].

V. CONCLUSIONS AND FUTURE DIRECTIONS

We have studied the existence and stability of bright and dark matter-wave solitons in Bose-Einstein condensates with spatially dependent, periodic scattering lengths. Our analysis was based on an analytically tractable model given by a Gross-Pitaevskii equation with a periodic, piecewise-constant, spatially inhomogeneous nonlinearity. In particular, we used techniques from the theory of perturbed Hamiltonian dynamical systems in order to obtain conditions for the "persistence" of the matter-wave solitons and analyze their linear stability. We thereby found that solitons must be
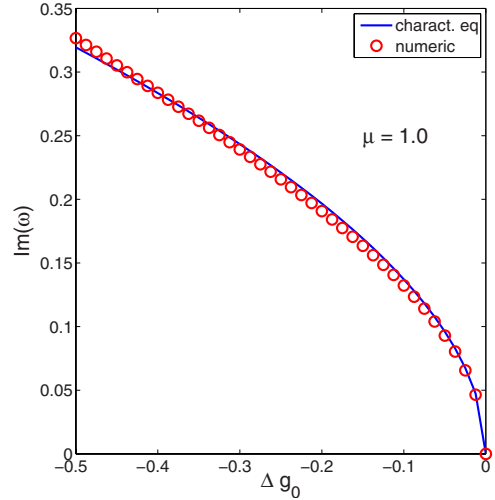
centered in one of the constant regions of the piecewise-constant coefficient of the nonlinearity (which is directly proportional to the atomic scattering length). We have shown that bright-soliton solutions are stable when localized in regions of maximal (absolute) nonlinearity and unstable when localized in regions of minimal (absolute) nonlinearity. This is consistent with the findings of earlier works on the NLS equation with periodic potentials (see, for example, Refs. [46,47,49]). In this situation, we also presented an approximate analytical technique (called "stitching") that allowed us to match the solution in a semianalytical fashion at the interfaces where the nonlinearity coefficient changes in order to obtain an accurate profile of the soliton in the presence of the spatial inhomogeneity. We applied a similar approach to dark matter-wave solitons (for which the translational eigenvalue is still responsible for the configurational stability) to show a rather different final result. Specifically, we showed that dark solitons centered at $\min[g(z)]$ feature a complex eigenvalue quartet, whereas the ones centered at $\max[g(z)]$ have a pair of unstable real eigenvalues. Therefore, both cases are unstable, but the former instability is oscillatory and the latter is purely exponential (typically with a larger growth rate). In all cases, we corroborated both the existence and linear stability results with corresponding numerical computations, which were in good agreement with our analytical findings.

It would be interesting to extend the present results to more complicated configurations. One interesting example along the lines of Ref. [49] might be to examine the competition of a piecewise-nonlinear and a piecewise-linear potential in one dimension. Another possibility would be to investigate the stitching between spatially extended solutions given by elliptic functions. Perhaps a more appealing example for a generalization of the present context would be to examine piecewise-constant nonlinearities in higher dimensions (with, for example, a piecewise-constant radial form or a piecewise-constant, square-lattice form) and determine the

stability of vortexlike and similar structures in the defocusing NLS. In the focusing case, it would also be interesting to determine whether such a nonlinearity could stabilize solitary waves (which would be given by piecewise generalizations of the Townes soliton) against collapse.

[1] C. J. Pethick and H. Smith, *Bose-Einstein Condensation in Dilute Gases*, 2nd ed. (Cambridge University Press, Cambridge, England, 2008).

[2] L. P. Pitaevskii and S. Stringari, *Bose-Einstein Condensation* (Oxford University Press, Oxford, 2003).

[3] K. E. Strecker, G. B. Partridge, A. G. Truscott, and R. G. Hulet, Nature (London) **417**, 150 (2002).

[4] L. Khaykovich, F. Schreck, G. Ferrari, T. Bourdel, J. Cubizolles, L. D. Carr, Y. Castin, and C. Salomon, Science **296**, 1290 (2002).

[5] S. L. Cornish, S. T. Thompson, and C. E. Wieman, Phys. Rev. Lett. **96**, 170401 (2006).

[6] S. Burger, K. Bongs, S. Dettmer, W. Ertmer, K. Sengstock, A. Sanpera, G. V. Shlyapnikov, and M. Lewenstein, Phys. Rev. Lett. **83**, 5198 (1999).

[7] J. Denschlag, J. E. Simsarian, D. L. Feder, C. W. Clark, L. A. Collins, J. Cubizolles, L. Deng, E. W. Hagley, K. Helmerson, W. P. Reinhardt, S. L. Rolston, B. I. Schneider, and W. D. Phillips, Science **287**, 97 (2000).

[8] B. P. Anderson, P. C. Haljan, C. A. Regal, D. L. Feder, L. A. Collins, C. W. Clark, and E. A. Cornell, Phys. Rev. Lett. **86**, 2926 (2001).

[9] Z. Dutton, M. Budde, Ch. Slowe, and L. V. Hau, Science **293**, 663 (2001).

[10] B. Eiermann, Th. Anker, M. Albiez, M. Taglieber, P. Treutlein, K.-P. Marzlin, and M. K. Oberthaler, Phys. Rev. Lett. **92**, 230401 (2004).

[11] *Emergent Nonlinear Phenomena in Bose-Einstein Condensates: Theory and Experiment*, edited by P. G. Kevrekidis, D. J. Frantzeskakis, and R. Carretero-González (Springer-Verlag, Berlin, 2008).

[12] P. G. Kevrekidis and D. J. Frantzeskakis, Mod. Phys. Lett. B **18**, 173 (2004).

[13] V. A. Brazhnyi and V. V. Konotop, Mod. Phys. Lett. B **18**, 627 (2004).

[14] I. Bloch, J. Phys. B **38**, S629 (2005); Nat. Phys. **1**, 23 (2005).

[15] O. Morsch and M. Oberthaler, Rev. Mod. Phys. **78**, 179 (2006).

[16] R. Folman, P. Krüger, J. Schmiedmayer, J. Denschlag, and C. Henkel, Adv. At., Mol., Opt. Phys. **48**, 263 (2002); J. Reichel, Appl. Phys. B: Lasers Opt. **74**, 469 (2002); J. Fortágh and C. Zimmermann, Science **307**, 860 (2005); Rev. Mod. Phys. **79**, 235 (2007).

[17] R. Grimm, M. Weidemüller, and Y. B. Ovchinnikov, Adv. At., Mol., Opt. Phys. **42**, 95 (2000).

[18] S. Hofferberth, I. Lesanovsky, B. Fischer, J. Verdu, and J. Schmiedmayer, Nat. Phys. **2**, 710 (2006); I. Lesanovsky, S. Hofferberth, J. Schmiedmayer, and P. Schmelcher, Phys. Rev. A **74**, 033619 (2006); I. Lesanovsky, T. Schumm, S. Hofferberth, L. M. Andersson, P. Krüger, and J. Schmiedmayer, *ibid.* **73**, 033619 (2006).

[19] T. Köhler, K. Goral, and P. S. Julienne, Rev. Mod. Phys. **78**, 1311 (2006).

[20] S. Inouye, M. R. Andrews, J. Stenger, H. J. Miesner, D. M. Stamper-Kurn, and W. Ketterle, Nature (London) **392**, 151 (1998); J. Stenger, S. Inouye, M. R. Andrews, H.-J. Miesner, D. M. Stamper-Kurn, and W. Ketterle, Phys. Rev. Lett. **82**, 2422 (1999); J. L. Roberts, N. R. Claussen, J. P. Burke, Jr., C. H. Greene, E. A. Cornell, and C. E. Wieman, *ibid.* **81**, 5109 (1998); S. L. Cornish, N. R. Claussen, J. L. Roberts, E. A. Cornell, and C. E. Wieman, *ibid.* **85**, 1795 (2000).

[21] F. K. Fatemi, K. M. Jones, and P. D. Lett, Phys. Rev. Lett. **85**, 4462 (2000); M. Theis, G. Thalhammer, K. Winkler, M. Hellwig, G. Ruff, R. Grimm, and J. H. Denschlag, *ibid.* **93**, 123001 (2004).

[22] M. Olshanii, Phys. Rev. Lett. **81**, 938 (1998).

[23] K. Günter, T. Stöferle, H. Moritz, M. Köhl, and T. Esslinger, Phys. Rev. Lett. **95**, 230401 (2005).

[24] J. Herbig, T. Kraemer, M. Mark, T. Weber, C. Chin, H. C. Nagerl, and R. Grimm, Science **301**, 1510 (2003); C. A. Regal, C. Ticknor, J. L. Bohn, and D. S. Jin, Nature (London) **424**, 47 (2003).

[25] M. Bartenstein, A. Altmeyer, S. Riedl, S. Jochim, C. Chin, J. H. Denschlag, and R. Grimm, Phys. Rev. Lett. **92**, 203201 (2004); T. Bourdel, L. Khaykovich, J. Cubizolles, J. Zhang, F. Chevy, M. Teichmann, L. Tarruell, S. J. J. M. F. Kokkelmans, and C. Salomon, *ibid.* **93**, 050401 (2004).

[26] F. Kh. Abdullaev, J. G. Caputo, R. A. Kraenkel, and B. A. Malomed, Phys. Rev. A **67**, 013605 (2003); H. Saito and M. Ueda, Phys. Rev. Lett. **90**, 040403 (2003); G. D. Montesinos, V. M. Pérez-García, and P. J. Torres, Physica D **191**, 193 (2004).

[27] P. G. Kevrekidis, G. Theocharis, D. J. Frantzeskakis, and B. A. Malomed, Phys. Rev. Lett. **90**, 230401 (2003); Z. X. Liang, Z. D. Zhang, and W. M. Liu, *ibid.* **94**, 050402 (2005); M. Matuszewski, E. Infeld, B. A. Malomed, and M. Trippenbach, *ibid.* **95**, 050403 (2005).

[28] S. K. Turitsyn, E. G. Turitsyna, S. B. Medvedev, and M. P. Fedoruk, Phys. Rev. E **61**, 3127 (2000).

[29] A. Wingen, K. H. Spatschek, and S. B. Medvedev, Phys. Rev.

E **68**, 046610 (2003).

[30] V. Zharnitsky and D. E. Pelinovsky, Chaos **15**, 037105 (2005).

[31] D. E. Pelinovsky, P. G. Kevrekidis, and D. J. Frantzeskakis, Phys. Rev. Lett. **91**, 240201 (2003); D. E. Pelinovsky, P. G. Kevrekidis, D. J. Frantzeskakis, and V. Zharnitsky, Phys. Rev. E **70**, 047604 (2004).

[32] P. G. Kevrekidis, D. E. Pelinovsky, and A. Stefanov, J. Phys. A **39**, 479 (2006).

[33] G. Theocharis, P. Schmelcher, P. G. Kevrekidis, and D. J. Frantzeskakis, Phys. Rev. A **72**, 033614 (2005).

[34] F. Kh. Abdullaev and M. Salerno, J. Phys. B **36**, 2851 (2003).

[35] M. I. Rodas-Verde, H. Michinel, and V. M. Pérez-García, Phys. Rev. Lett. **95**, 153903 (2005); A. V. Carpentier, H. Michinel, M. I. Rodas-Verde, and V. M. Pérez-García, Phys. Rev. A **74**, 013619 (2006).

[36] G. Theocharis, P. Schmelcher, P. G. Kevrekidis, and D. J. Frantzeskakis, Phys. Rev. A **74**, 053614 (2006).

[37] J. Garnier and F. Kh. Abdullaev, Phys. Rev. A **74**, 013604 (2006).

[38] G. Dong, B. Hu, and W. Lu, Phys. Rev. A **74**, 063601 (2006).

[39] Yu. V. Bludov, V. A. Brazhnyi, and V. V. Konotop, Phys. Rev. A **76**, 023603 (2007).

[40] P. Niarchou, G. Theocharis, P. G. Kevrekidis, P. Schmelcher, and D. J. Frantzeskakis, Phys. Rev. A **76**, 023615 (2007).

[41] F. Kh. Abdullaev and J. Garnier, Phys. Rev. A **72**, 061605(R) (2005).

[42] H. Sakaguchi and B. A. Malomed, Phys. Rev. E **72**, 046610 (2005); M. A. Porter, P. G. Kevrekidis, B. A. Malomed, and D. J. Frantzeskakis, Physica D **229**, 104 (2007); F. Kh. Abdullaev, A. Abdumalikov, and R. Galimzyanov, Phys. Lett. A **367**, 149 (2007).

[43] Y. V. Bludov and V. V. Konotop, Phys. Rev. A **74**, 043616 (2006).

[44] M. T. Primatarowa, K. T. Stoychev, and R. S. Kamburova, Phys. Rev. E **72**, 036608 (2005).

[45] V. M. Pérez-García, e-print arXiv:nlin-sys/0612028.

[46] G. Fibich, Y. Sivan, and M. I. Weinstein, Physica D **217**, 31 (2006).

[47] Y. Sivan, G. Fibich, and M. I. Weinstein, Phys. Rev. Lett. **97**, 193902 (2006).

[48] J. Belmonte-Beitia, V. M. Pérez-García, V. Vekslerchik, and P. J. Torres, Phys. Rev. Lett. **98**, 064102 (2007).

[49] Z. Rapti, P. G. Kevrekidis, V. V. Konotop, and C. K. R. T. Jones, J. Phys. A **40**, 14151 (2007).

[50] F. Kh. Abdullaev, Yu. V. Bludov, S. V. Dmitriev, P. G. Kevrekidis, and V. V. Konotop, Phys. Rev. E **77**, 016604 (2008).

[51] S. Eriksson, M. Trupke, H. F. Powell, D. Sahagun, C. D. J. Sinclair, E. A. Curtis, B. E. Sauer, E. A. Hinds, Z. Moktadir, C. O. Gollasch, and M. Kraft, Eur. Phys. J. D **35**, 135 (2005).

[52] A. Shevchenko, M. Heiliö, T. Lindvall, A. Jaakkola, I. Tittonen, M. Kaivola, and T. Pfau, Phys. Rev. A **73**, 051401(R) (2006).

[53] Y. Kominis, Phys. Rev. E **73**, 066619 (2006); Y. Kominis and K. Hizanidis, Opt. Lett. **31**, 2888 (2006); Y. Kominis, A. Papadopoulos, and K. Hizanidis, Opt. Express **15**, 10041 (2007).

[54] T. Kapitula, P. G. Kevrekidis, and B. Sandstede, Physica D **195**, 263 (2004); T. Kapitula and P. G. Kevrekidis, J. Phys. A **37**, 7509 (2004).

[55] D. E. Pelinovsky and P. G. Kevrekidis, ZAMP **59**, 559 (2008).

[56] V. M. Pérez-García, H. Michinel, and H. Herrero, Phys. Rev. A **57**, 3837 (1998); A. D. Jackson, G. M. Kavoulakis, and C. J. Pethick, *ibid.* **58**, 2417 (1998).

[57] N. G. Parker, N. P. Proukakis, C. F. Barenghi, and C. S. Adams, J. Phys. B **37**, S175 (2004); G. Theocharis, D. J. Frantzeskakis, P. G. Kevrekidis, R. Carretero-González, and B. A. Malomed, Math. Comput. Simul. **69**, 537 (2005).

[58] M. Johansson and Yu. S. Kivshar, Phys. Rev. Lett. **82**, 85 (1999).